Pergamon

Int. J. Multiphase Flow Vol. 21, No. 6, pp. 1073–1089, 1995

0301-9322(95)00039-9
0301-9322/95 $9.50 + 0.00

RELATIONSHIPS BETWEEN DISTRIBUTIONS OF CHORD LENGTHS AND DISTRIBUTIONS OF BUBBLE SIZES INCLUDING THEIR STATISTICAL PARAMETERS

W. LIU and N. N. CLARK
Department of Mechanical and Aerospace Engineering, West Virginia University, Morgantown, WV 26506, U.S.A.

(Received 19 December 1994; in revised form 26 April 1995)

Abstract—The performance of fluidized beds is strongly influenced by bubble behavior. Among various hydrodynamic properties, bubble size distributions are of prime concern, but in practice, bubble size is not readily measured. When a probe is used to determine bubble size, it intersects a bubble with a chord length other than the largest vertical dimension. The relationships between the size distribution of bubbles in the bed, the size distribution of bubbles touching the probe and the distribution of chord lengths must be resolved for correct interpretation of probe signals. A method for translating statistical parameters, namely mean and standard deviation of chord lengths to mean and standard deviation of bubble sizes, and an approach to infer the size distribution of bubbles touching the probe and the size distribution of bubbles in the bed system by using the distribution of chord lengths measured by a probe in closed form are proposed for the first time.

Key Words: two-phase (flow), bubble, chord length, shape, size distribution, geometric probability, gas–liquid(flow), fluidization

INTRODUCTION

Fluidized beds and bubble columns are employed in a number of industrial processes because these beds have advantages, such as high rates of heat and mass transfer, due to effective contact between the phases (Epstein 1981). Bubble characteristics strongly influence hydrodynamics of multiphase beds and determine the performance of fluidized bed reactors and combustors. Among various hydrodynamic properties, bubble sizes and their distributions are of prime concern, as they are directly responsible for the behavior of other hydrodynamic properties such as flow patterns, solids mixing, gas–liquid interfacial area and mass transfer between the phases. However, it is very difficult to determine the size distribution of bubbles present in a fluidized bed in which bubbles rise from a distributor in a swarm and grow in size as they are rising through the bed. Nevertheless, bubble sizes can be characterized by chord lengths of bubbles pierced by a probe, which are easily measured. Previous work on converting the distribution of chord lengths to the size distribution of bubbles in numerical form has demonstrated an instability problem and is cumbersome (Clark & Turton 1988).

This paper discusses the relationships between the size distribution of bubbles in the bed, the size distribution of bubbles touching the probe and the distribution of measured chord lengths, proposes a method for inferring statistical parameters the mean and standard deviation of bubble sizes from the mean and standard deviation of chord lengths and provides an approach to infer the size distribution of bubbles touching the probe and the size distribution of bubbles in the bed system in analytical form by using the distribution of chord lengths measured by the probe.

LITERATURE REVIEW

There is a body of literature concerned with the relationships between bubble sizes and chord lengths in two-phase systems including gas–liquid mixtures and fluid bed bubble and dense phase mixtures. Geometrical probability concepts offer an elegant solution to the problem. Werther (1974a, b) provided the first analysis of the relationship between the distributions of chord lengths and the local bubble sizes. Lim *et al.* (1990a, b) used a digital image analysis technique with the aid of a video camera to obtain chord lengths and several size parameters of bubbles intersected at an "imaginary" probe in a thin, transparent two-dimensional fluidized bed. However, two-dimensional beds are not generally representative of the hydrodynamics in larger three-dimensional beds. Clark & Turton (1988) proposed forward and backward transforms relating chord lengths to bubble sizes for a variety of bubble shapes encountered in different multiphase flows, and Turton & Clark (1989) extended this technique to the case of spherical cap bubbles encountered in fluid beds with bubble rise velocity depending on bubble size. However, instability was observed with the backward transform when a small number of bubble measurement events was used to infer bubble size distributions. Irregular and even negative values of bubble population in a specific size range could result from too many size range bins or too few bubbles.

There are also several papers analyzing the relationships between average of bubble sizes and average of chord lengths. Gunn & Al-Dorri (1985) discussed that relationship for ellipsoidal bubbles in gas–liquid bed. Chan *et al.* (1987) and Weimer *et al.* (1985) also provided an approximate relationship between averages of bubble sizes and chord lengths for spherical bubbles.

Probes are effective tools for the study and measurement of bubble sizes in a fluidized bed system. There are several types of probes, such as optical, resistance/impedance, capacitance or dual hydrostatic pressure probes (Meernik & Yuen 1986a, b; Burgess *et al.* 1981; Werther & Molerus 1973; Atkinson & Clark 1986b) that can be used to measure chord lengths of bubbles. General reviews of fluidized bed probes were presented by Cheremisinoff (1986) and Atkinson & Clark (1986a). In this paper the "imaginary" probe gathering chord length data could work on any one of a number of principles and the basic probe signal processing will not be discussed.

THEORY

Consider a swarm of gas bubbles rising in a liquid or dense fluidized medium. A probe is operated amidst the bubbles, which are assumed to be uniformly distributed throughout the system for this analysis. The size distribution of bubbles in the bed system and the size distribution of bubbles touching the problem can be described by the probability functions $P_s(R)$ and $P_p(R)$, respectively. They differ because statistically the probe is more likely to intersect a large bubble than a small bubble. In measurement, the probe does not always intersect a bubble at its center. A chord length smaller than the largest vertical bubble dimension is typically measured. The chord length distribution not only is determined by bubble size distributions $P_p(R)$ or $P_s(R)$, but also is related to bubble shape.

Bubble shapes and chord lengths

There are several axisymmetric geometric shapes used to represent bubbles. Two typical models (Clark & Turton 1988) are employed in this paper.

(i) The ellipsoidal shape including spheroid is usually used to describe bubbles in gas–liquid systems with parameters, R radius on the larger horizontal axes and α $(0 < \alpha \leqslant 1)$ a shape factor given by the ratio of the minor (vertical) axis to the two major (horizontal) axes. This model is shown in figure 1(a).

(ii) The truncated ellipsoidal shape is used to represent bubbles in fluidized beds. These are termed "spherical cap" bubbles (Werther 1974a) as shown in figure 1(b). One more parameter is needed to describe the bubble shape, namely the truncation coefficient K, often used as $Q = \sqrt{1 - K^2}$.

During measurement, the probe intersects a bubble with a chord length other than the largest vertical length, whatever probe is used and whatever bubble shape is assumed. A chord length pierced by the probe is determined by the horizontal distance r between the center of bubble and the probe tip, as well as bubble shape and size. Consider that bubbles rise in the bed system vertically. The chord length y pierced by the probe for an elliposidally shaped bubble is

$$y = 2\alpha\sqrt{R^2 - r^2} \qquad [1]$$

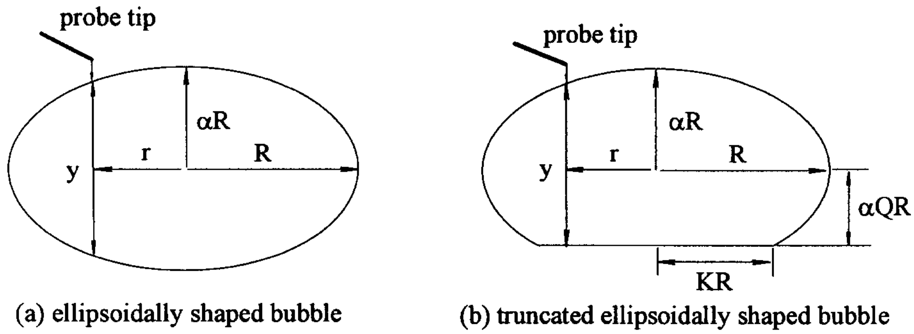

Figure 1. Bubble models represented by the ellipsoidal shape and the truncated ellipsoidal shape showing vertical chord length pierced by the probe tip.

For a truncated ellipsoid, there are two cases: when $0 \leqslant r \leqslant KR$, the chord length is

$$y = \alpha\sqrt{R^2 - r^2} + \alpha QR \qquad [2a]$$

and when $KR \leqslant r \leqslant R$, the chord length is the same as that for the ellipsoid,

$$y = 2\alpha\sqrt{R^2 - r^2} \qquad [2b]$$

A large number of bubbles with size distribution $P_p(R)$ intersect the probe to produce a chord length distribution $P_c(y)$. The chord lengths are known experimentally from a set of "pierced times" if the bubble rise velocity is known at the time of signal processing (Turton & Clark 1989).

Distributions of bubble sizes and chord lengths

For a certain type of size distribution of bubbles in the bed system, there is a corresponding size distribution of bubbles touching the probe and a chord length distribution. Assume that the probe tip is in the center of the system with the effective radius of the system set at R_{max} (the largest horizontal radius of bubbles in the system). The ratio of the number of bubbles with a specific radius R, which touch the probe, versus the number of bubbles of the same size which are in the column is,

$$\frac{P(R)}{P_s(R)} = \frac{\pi R^2}{\pi R^2_{max}} = \frac{R^2}{R^2_{max}}$$

then

$$P(R) = \frac{R^2}{R^2_{max}} P_s(R) \qquad [3]$$

where $P(R)$ is a probability of bubbles intersected by the probe. This concept has been expressed by Clark & Turton (1988).

The probability density function of the sizes of bubbles which are intersected by the probe, i.e. the normalized $P(R)$, is defined as,

$$P_p(R) = \frac{P(R)}{\int_{-\infty}^{\infty} P(R)\,\mathrm{d}R} \qquad [4]$$

Substituting [3] into [4], yields

$$P_p(R) = \frac{R^2 P_s(R)}{\int_{-\infty}^{\infty} R^2 P_s(R)\,\mathrm{d}R} = \frac{R^2 P_s(R)}{\text{the second moment } P_s(R)} \qquad [5]$$

Equation [5] indicates that the $P_p(R)$ (the size distribution of bubbles touching the probe) can be found from $P_s(R)$ (the size distribution of bubbles in the bed). When $P_p(R)$ is known, $P_s(R)$ can be represented as,

$$P_s(R) = \frac{R^2_{max}}{R^2} P(R) = \frac{R^2_{max}}{R^2} P_p(R) \int_{-\infty}^{\infty} P(R)\,\mathrm{d}R \qquad [6]$$

Because $\int_{-\infty}^{\infty} P_s(R)\,dR = 1$, then

$$\int_{-\infty}^{\infty} P(R)\,dR = \frac{1}{\displaystyle\int_{-\infty}^{\infty} \frac{R_{max}^2}{R^2} P_p(R)\,dR} \qquad [7]$$

substituting [7] into [6], yields

$$P_s(R) = \frac{P_p(R)/R^2}{\displaystyle\int_{-\infty}^{\infty} \frac{P_p(R)}{R^2}\,dR} \qquad [8]$$

The above equation provides a way to find the probability density function of bubbles in the bed system, when $P_p(R)$ is known. Equations [5] and [8] demonstrate that measurement of bubbles favors bubbles of larger average size than the average size in the bed system.

The conditional probability density function for a chord length y pierced by the probe from bubbles with a specific size R can be derived as the following, by using the geometrical probability approach. One needs to consider the probability that the chord length will lie between a value y and $y + dy$, given that the radius lies between r and dr.

$$P_c(y/R) = \frac{2r}{R^2}\left|\frac{dr}{dy}\right| \qquad [9]$$

In this paper, all the bubbles are assumed to be geometrically similar and can be characterized by a single size parameter along with certain shape parameters. The probability of chord lengths occurring is readily deduced as follows for bubbles touching the probe with probability density function $P_p(R)$,

$$P_c(y) = \int_{-\infty}^{\infty} P_c(y/R) P_p(R)\,dR \qquad [10]$$

The value of $|dr/dy|$ can be found from [1] for the ellipsoidally shaped bubbles and from [2] for the truncated ellipsoidally shaped bubbles (Clark & Turton 1988). For the ellipsoidally shaped bubble model, the conditional probability density function can be written as,

for $0 \leqslant y \leqslant 2\alpha QR$

$$P_c(y/R) = \frac{y}{2\alpha^2 R^2} \qquad [11a]$$

else

$$P_c(y/R) = 0 \qquad [11b]$$

and the distribution of chord lengths can be written as,

$$P_c(y) = \int_{y/2\alpha}^{\infty} \frac{y}{\alpha^2 R^2} P_p(R)\,dR \qquad [12]$$

For the truncated ellipsoidally shaped bubble model, the conditional probability density function of chord lengths can be written as,

for $0 \leqslant y \leqslant 2\alpha QR$

$$P_c(y/R) = \frac{y}{2\alpha^2 R^2} \qquad [13a]$$

and for $2\alpha QR \leqslant y \leqslant \alpha(1 + Q)R$

$$P_c(y/R) = \frac{2}{\alpha^2 R^2}(y - \alpha QR) \qquad [13b]$$

else

$$P_c(y/R) = 0 \qquad [13c]$$

and the distribution of chord lengths can be written as,

$$\text{for } 0 \leqslant y \leqslant \alpha Q R_{\max}\ P_c(y) = \int_{y/2\alpha Q}^{\infty} \frac{y}{2\alpha^2 R^2} P_p(R)\,dR + \int_{y/\alpha(1+Q)}^{y/2\alpha Q} \frac{2}{\alpha^2 R^2}(y - \alpha Q R) P_p(R)\,dR \quad [14a]$$

$$\text{for } y \geqslant 2\alpha Q R_{\max}\ P_c(y) = \int_{y/\alpha(1+Q)}^{\infty} \frac{2}{\alpha^2 R^2}(y - \alpha Q R) P_p(R)\,dR \quad [14b]$$

Equations [12] and [14] provide techniques for deducing the distribution of chord lengths for a given size distribution of bubbles touching the problem, $P_p(R)$ and ultimately for a given size distribution of bubbles in the bed, $P_s(R)$.

Two specific probability functions

Gamma and Rayleigh probability funtions start from non-negative values and can often be fitted closely to the distributions of bubble sizes and chord lengths. The former probability function was used by Lim & Agarwal (1990) in fitting their measured data. The Rayleigh probability function has a similar shape to the Gamma function and is simpler in form. If the size distribution of bubbles in the bed is described by one of those distributions, one may seek the size distribution of bubbles touching the probe and the distribution of chord lengths.

Case I. Assume $P_s(R)$, the size distribution of bubbles in the bed, is described by a Gamma function with adjustable parameters q and λ as follows,

$$P_s(R) = \frac{\lambda^q}{\Gamma(q)} R^{q-1} e^{-\lambda R} \quad (R \geqslant 0, q > 0, \lambda > 0) \quad [15]$$

then, the size distribution of bubbles touching the probe can be readily found as,

$$P_p(R) = \frac{R^2 P_s(R)}{\text{the second moment of } P_s(R)} = \frac{R^2 \dfrac{\lambda^q}{\Gamma(q)} R^{q-1} e^{-\lambda R}}{(q+1)q/\lambda^2} = \frac{\lambda^{q+2}}{\Gamma(q+2)} R^{q+1} e^{-\lambda R} \quad [16]$$

Equation [16] indicates that $P_p(R)$, the size distribution of bubbles touching the probe is also a Gamma probability function with the same λ, only the parameter q is changed to $q + 2$.

For the ellipsoidally shaped bubbles, the distribution of chord lengths $P_c(y)$ can be written as,

$$\begin{aligned} P_c(y) &= \int_{y/2\alpha}^{\infty} \frac{y}{2\alpha^2 R^2} \cdot \frac{\lambda^{q+2}}{\Gamma(q+2)} R^{q+1} e^{-\lambda R}\,dR \\ &= -\frac{y\lambda^{q+1}}{2\alpha^2 \Gamma(q+2)} R^{q-1} e^{-\lambda R}\Big|_{y/2\alpha}^{\infty} + \frac{y\lambda^{q+1}(q-1)}{2\alpha^2 \Gamma(q+2)} \int_{t/2\alpha}^{\infty} R^{q-2} e^{-\lambda R}\,dR \\ &= \frac{2q}{q(q+1)} \frac{(\lambda/2\alpha)^{q+1}}{\Gamma(q+1)} y^q e^{-(\lambda/2\alpha)y} \\ &\quad + \frac{y\lambda^{q+1}(q-1)}{2\alpha^2 q(q+1)\Gamma(q)} \int_{y/2\alpha}^{\infty} R^{q-2} e^{-\lambda R}\,dR \end{aligned}$$

When q is an integer greater than zero, then

$$P_c(y) = \sum_{i=1}^{q} \frac{2i}{q(q+1)} \frac{(\lambda/2\alpha)^{i+1}}{\Gamma(i+1)} y^i e^{-(\lambda/2\alpha)y} \quad [17]$$

This means that $P_c(y)$ is the sum of a set of Gamma probability functions with weighting coefficients $2i/(q+1)q$.

Case II. When $P_s(R)$, the size distribution of bubbles in the bed, is described by a Rayleigh probability function with parameter μ as follows,

$$P_s(R) = \frac{R}{\mu^2} e^{-R^2/2\mu^2} \quad (R \geqslant 0, \mu > 0) \quad [18]$$

then, the size distribution of bubbles touching the probe $P_p(R)$ can be written as,

$$P_p(R) = \frac{R^2 \dfrac{R}{\mu^2} e^{-R^2/2\mu^2}}{\left(\sqrt{\dfrac{\pi}{2}}\mu\right)^2 + \dfrac{4-\pi}{2}\mu^2} = \frac{R^3}{2\mu^4} e^{-R^2/2\mu^2} \qquad [19]$$

The distribution of chord lengths for ellipsoidally shaped bubbles can be written as,

$$P_p(y) = \int_{y/2\alpha}^{\infty} \frac{y}{2\alpha^2 R^2} \frac{R^3}{2\mu^4} e^{-R^2/2\mu^2} \, dR = \frac{y}{(2\alpha\mu)^2} e^{-y^2/2(2\alpha\mu)^2} \qquad [20]$$

From [20], it is not difficult to find that the distribution of chord lengths is also a Rayleigh distribution with parameter $2\alpha\mu$. Therefore, it can be concluded that if the measured chord length data can be fitted by a Rayleigh probability function, the size distribution of bubbles in the bed can be quickly inferred as a Rayleigh distribution with the parameter which is the parameter of the Rayleigh probability function of chord lengths divided by 2α.

Figures 2 and 4 show size distributions of bubbles in the bed, $P_s(R)$, which are Gamma and Rayleigh distributions with varying parameters λ, q and μ. Also shown are corresponding size distributions of bubbles touching the probe, $P_p(R)$, and distributions of chord lengths, $P_c(y)$ for the ellipsoidally shaped bubbles with a shape factor $\alpha = 0.6$. Figure 3 shows that $P_s(R)$ is a Gamma probability function with $\lambda = 3$ and $q = 4$, and related curves for $P_p(R)$ and $P_c(y)$ for shape factor $\alpha = 0.5$ and 1, respectively.

For truncated ellipsoidal shape bubbles, the integration required to evaluate $P_c(y)$ becomes far more complex, due to segmentation of the probability, and an analytic solution is not offered here.

Statistical analysis

In this section the relationship of statistical parameters (mean and standard deviation) between chord lengths and bubble sizes is analyzed. The following techniques provide an approach for rapid translation from one distribution to the other. No specific form of the distribution is prescribed in this general case.

The mean of the size distribution of bubbles touching the probe is defined as M_{pR}, that is,

$$M_{pR} = \int_0^{\infty} R P_p(R) \, dR \qquad [21]$$

and the square of standard deviation of the size distribution of bubbles touching the probe is defined as σ_{pR}^2, that is,

$$\alpha_{pR}^2 = \int_0^{\infty} R^2 P_p(R) \, dR - M_{pR}^2 \qquad [22]$$

The mean of chord lengths M_{cye} for ellipsoidally shaped bubbles can be written as,

$$\begin{aligned} M_{cye} &= \int_0^{\infty} y P_c(y) \, dy = \int_0^{\infty} y \left(\int_{y/2\alpha}^{\infty} \frac{y}{2\alpha^2 R^2} P_p(R) \, dR \right) dy \\ &= \int_0^{\infty} \left(\int_0^{2\alpha R} \frac{y^2}{2\alpha^2 R^2} P_p(R) \, dy \right) dR = \frac{4\alpha}{3} \int_0^{\infty} R P_p(R) \, dR = \frac{4\alpha}{3} M_{pR} \qquad [23] \end{aligned}$$

and the square of standard deviation of chord lengths α_{cye}^2 can be written as,

$$\begin{aligned} \sigma_{cye}^2 &= \int_0^{\infty} y^2 P_c(y) \, dy - (M_{cye})^2 = \int_0^{\infty} y^2 \left(\int_{y/2\alpha}^{\infty} \frac{y}{2\alpha^2 R^2} P_p(R) \, dR \right) dy - (M_{cye})^2 \\ &= \int_0^{\infty} \left(\int_0^{2\alpha R} \frac{y^3}{2\alpha^2 R^2} P_p(R) \, dy \right) dR - (M_{cye})^2 = 2\alpha^2 \int_0^{\infty} R^2 P_p(R) \, dR - (M_{cye})^2 \\ &= 2\alpha^2 \left(\int_0^{\infty} R^2 P_p(R) \, dR - M_{pR}^2 \right) + 2\alpha^2 M_{pR}^2 - \left(\frac{4\alpha}{3} M_{pR} \right)^2 \end{aligned}$$

then

$$\sigma_{cye}^2 = 2\alpha^2 \sigma_{pR}^2 + \frac{2\alpha^2}{9} M_{pR}^2 \qquad [24]$$

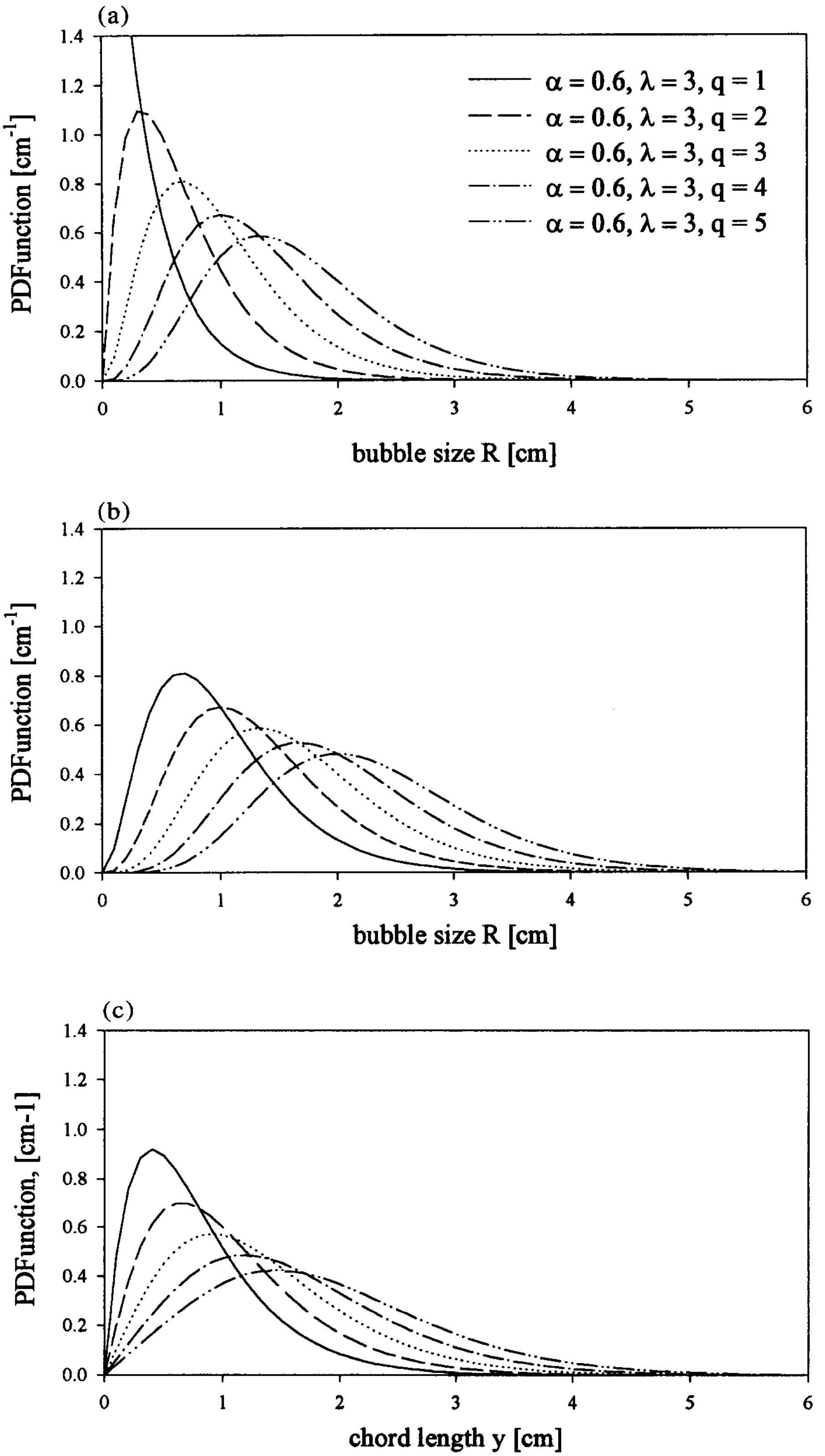

Figure 2. Size distributions in the bed represented by Gamma probability functions and corresponding size distributions of bubbles touching the probe and distributions of chord lengths. (a) $P_s(R)$ size distributions of bubbles in the bed—Gamma distributions; (b) $P_p(R)$ size distributions of bubbles touching the probe—Gamma distributions; (c) $P_c(y)$ distributions of chord lengths for ellipsoidally shaped bubbles—sum of Gamma distributions with weighting coefficients.

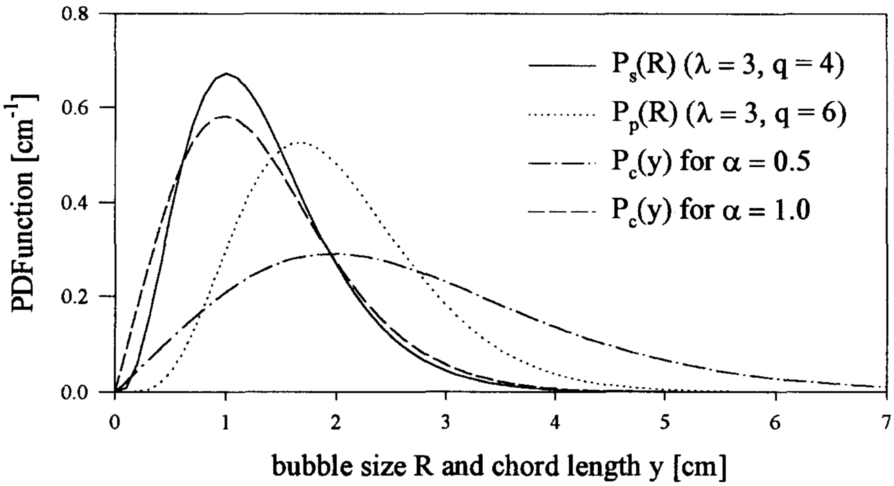

Figure 3. Size distribution in the bed represented by a Gamma probability function and corresponding size distribution of bubbles touching the probe and distributions of chord lengths for ellipsoidally shaped bubbles with different bubble factors.

Equation [23] reveals that the mean of chord lengths, M_{cye} is directly proportional to the mean size of the bubbles touching the probe, M_{pR} which is expected for reasons of geometric similarity. Equation [24] indicates that the square of the standard deviation (variance) of chord lengths, α^2_{cye} is proportional to the square of the standard deviation of sizes of bubbles touching the probe, σ^2_{pR} and also to the square of M_{pR}. The coefficients in both equations are independent of the distribution of chord lengths and the size distribution of bubbles touching the probe, and only related to the bubble shape factor α.

Based on the same approach, the mean M_{cyt} and the square of standard deviation of chord lengths α^2_{cyt} for truncated ellipsoidally shaped bubbles can be derived as follows,

$$
\begin{aligned}
M_{cyt} &= \int_0^\infty yP_c(y)\,dy = \int_0^{2\alpha QR_{max}} y\left(\int_{y/2\alpha Q}^{R_{max}} \frac{y}{2\alpha^2R^2}P_p(R)\,dR + \int_{y/\alpha(1+Q)}^{y/2\alpha Q} \frac{2}{\alpha^2R^2}\right. \\
&\quad \left.\times (y-\alpha QR)P_p(R)\,dR\right)dy + \int_{2\alpha R_{max}}^{\alpha(1+Q)R_{max}} y\left(\int_{y/\alpha(1+Q)}^{R_{max}} \frac{2}{\alpha^2R^2}(y-\alpha QR)P_p(R)\,dR\right)dy \\
&= \int_0^{2\alpha QR_{max}} y\left(\int_{y/2\alpha Q}^{R_{max}} \frac{4\alpha QR-3y}{2\alpha^2R^2}P_p(R)\,dR\right)dy + \int_0^{\alpha(1+Q)R_{max}} y\left(\int_{y/\alpha(1+Q)}^{R_{max}} \frac{2}{\alpha^2R^2}\right. \\
&\quad \left.\times (y-\alpha QR)P_p(R)\,dR\right)dy \\
&= \int_0^\infty \left(\int_0^{2\alpha QR} \frac{4\alpha QRy-3y^2}{2\alpha^2R^2}P_p(R)\,dy\right)dR \\
&\quad + \int_0^\infty \left(\int_0^{\alpha(1+Q)R} \frac{2}{\alpha^2R^2}(y^2-\alpha QRy)P_p(R)\,dy\right)dR
\end{aligned}
$$

then

$$M_{cyt} = (\tfrac{2}{3}\alpha(1+Q)^3 - \alpha Q(1+Q)^2)M_{pR} \qquad [25]$$

and

$$\sigma^2_{cyt} = \int_0^\infty y^2P_c(y)\,dR - M_{cyt}$$

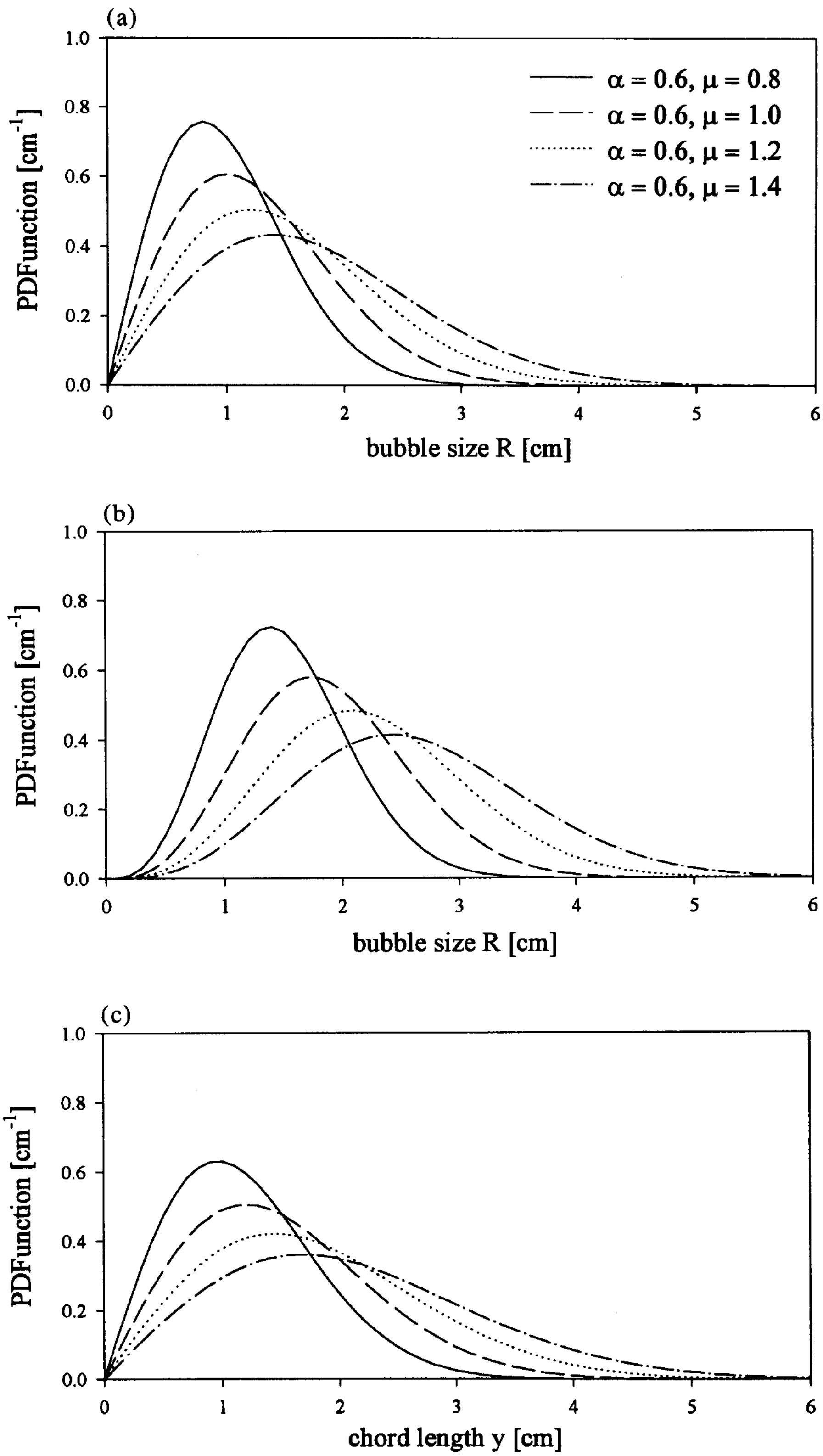

Figure 4. Size distributions in the bed represented by Rayleigh probability functions and corresponding size distributions of bubbles touching the probe and distributions of chord lengths. (a) $P_s(R)$ size distributions of bubbles in the bed—Rayleigh distributions; (b) $P_p(R)$ size distributions of bubbles touching the probe; (c) $P_c(y)$ distributions of chord lengths for ellipsoidally shaped bubbles—Rayleigh distributions.

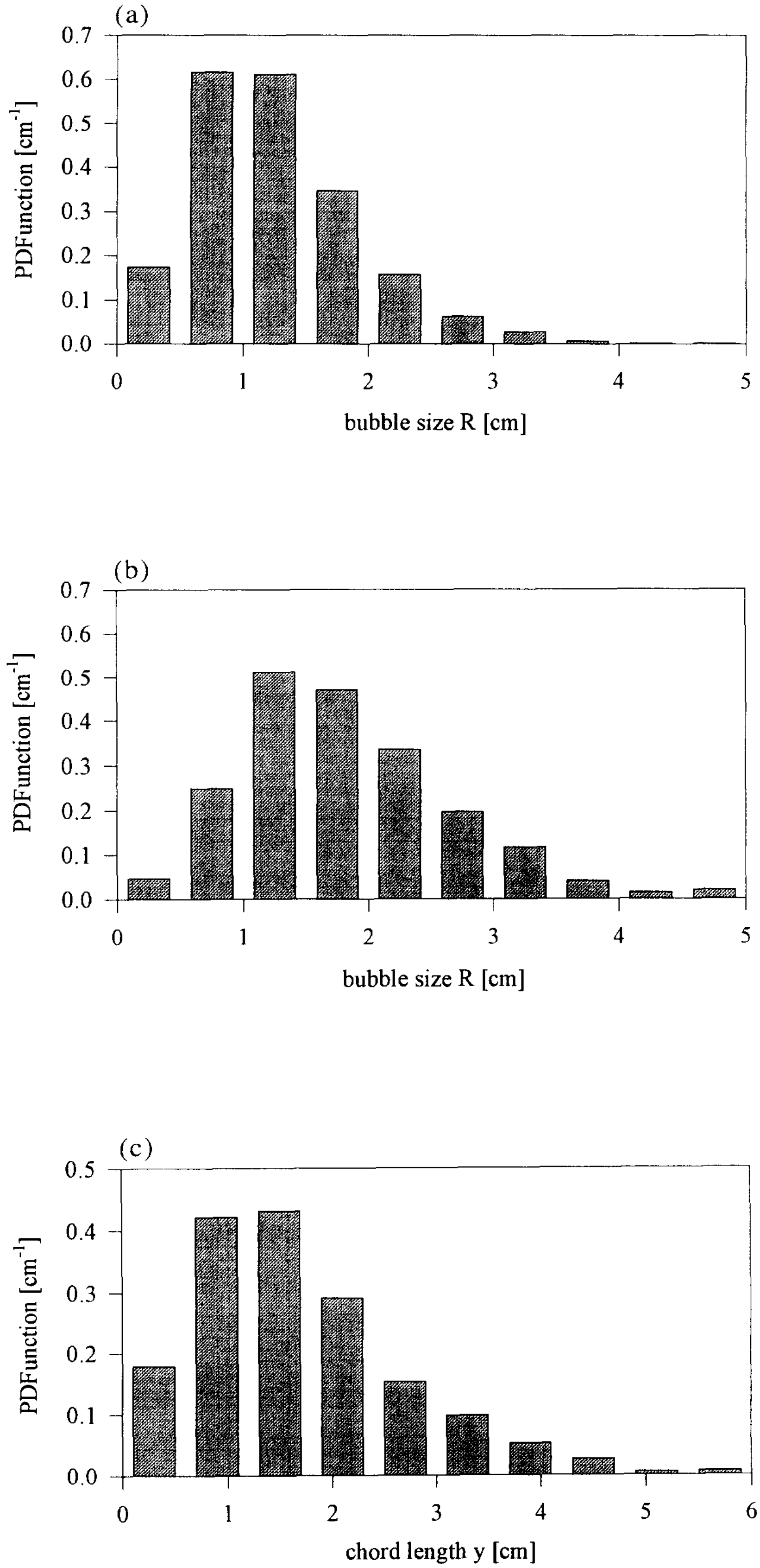

Figure 5 (a), (b) and (c) *Caption opposite*

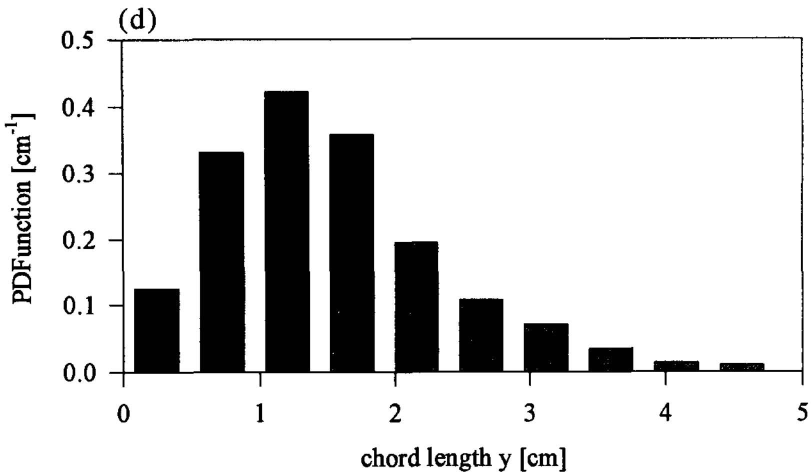

Figure 5(d)

Figure 5. Distributions of bubble sizes and chord lengths simulated for a given size distribution of bubbles in the bed—the Gamma probability function with parameters $q = 4$, $\lambda = 2.8$ and bubble shape factor $\alpha = 0.6$ for either ellipsoidally shaped bubbles or truncated ellipsoidally shaped bubbles with the truncation coefficient $K = 0.8$ (a) Size distribution of bubbles in the bed; (b) size distribution of bubbles touching the probe; (c) distribution of chord lengths of ellipsoidally shaped bubbles; (d) distribution of chord lengths of truncated ellipsoidally shaped bubbles.

thus,

$$\sigma_{cyt}^2 = (\tfrac{1}{2}\alpha^2(1+Q)^4 - \tfrac{2}{3}\alpha^2 Q(1+Q)^3 - \tfrac{2}{3}\alpha^2 Q^4)\sigma_{pR}^2 + (\tfrac{1}{2}\alpha^2(1+Q)^4 - \tfrac{2}{3}\alpha^2 Q(1+Q)^3 - \tfrac{2}{3}\alpha^2 Q^4 - (\tfrac{2}{3}\alpha(1+Q)^3 - \alpha Q(1+Q)^2)^2)M_{pR}^2 \quad [26]$$

Equations [25] and [26] are analogous to [23] and [24]. The coefficients in [25] and [26] are also related to the truncation coefficient K or Q used to describe bubble shape, besides being related to the ellipsoidal shape factor α.

The significance of those equations in practice is that when chord lengths are measured, the mean chord length M_{cye} and standard deviation α_{cye} for ellipsoidal shape bubbles or the mean chord length M_{cyt} and standard deviation α_{cyt} for truncated ellipsoidal shape bubbles can be found based on the measured data, then, the mean M_{pR} and standard deviation α_{pR} of bubbles touchings the probe are readily found by using [23] and [24] or [25] and [26]. It is worth mentioning that [25] equals [23] and [26] equals [24], respectively, when the truncated coefficient K equals 0, that is Q is 1, representing no truncation. Thus, [25] and [26] are a more general form for the bubbles.

Simulation

A Monte-Carlo simulation method was used to generate bubbles synthetically around an imaginary probe. Two sets of random numbers (10,000 bubbles in the bed system) of bubble sizes R were generated based on specified functions for $P_s(R)$ which were a Gamma distribution with parameters $q = 4$ and $\lambda = 2.8$, and a Rayleigh distribution with parameter $\mu = 1.4$, respectively. Bubbles were uniformly distributed through the bed. Bubble shape factor α was 0.6 for either ellipsoidally shaped bubbles or truncated ellipsoidally shaped bubbles. The truncation coefficient of truncated ellipsoidally shaped bubbles, K was 0.8, i.e. $Q = 0.6$. The generated size distributions of bubbles in the bed and touching the probe and distributions of chord lengths pierced by the imaginary probe, which were calculated by using [1] or [2], are shown in figures 5 and 6. Means and standard deviations of bubbles in the bed and touching the probe and of chord lengths in simulation are listed in table 1 along with their theoretical values. Means and standard deviations of bubbles touching the probe calculated from [23] to [26] are listed in table 2.

In table 1 theoretical values were found from [15], [16] and [17] for $P_s(R)$ given by a Gamma distribution with parameters $\lambda = 2.8$, $q = 4$, and from [18], [19] and [20] for $P_s(R)$ given by a Rayleigh distribution with parameter $\mu = 1.4$. The bubble shape factor α is 0.6 for both ellipsoidally

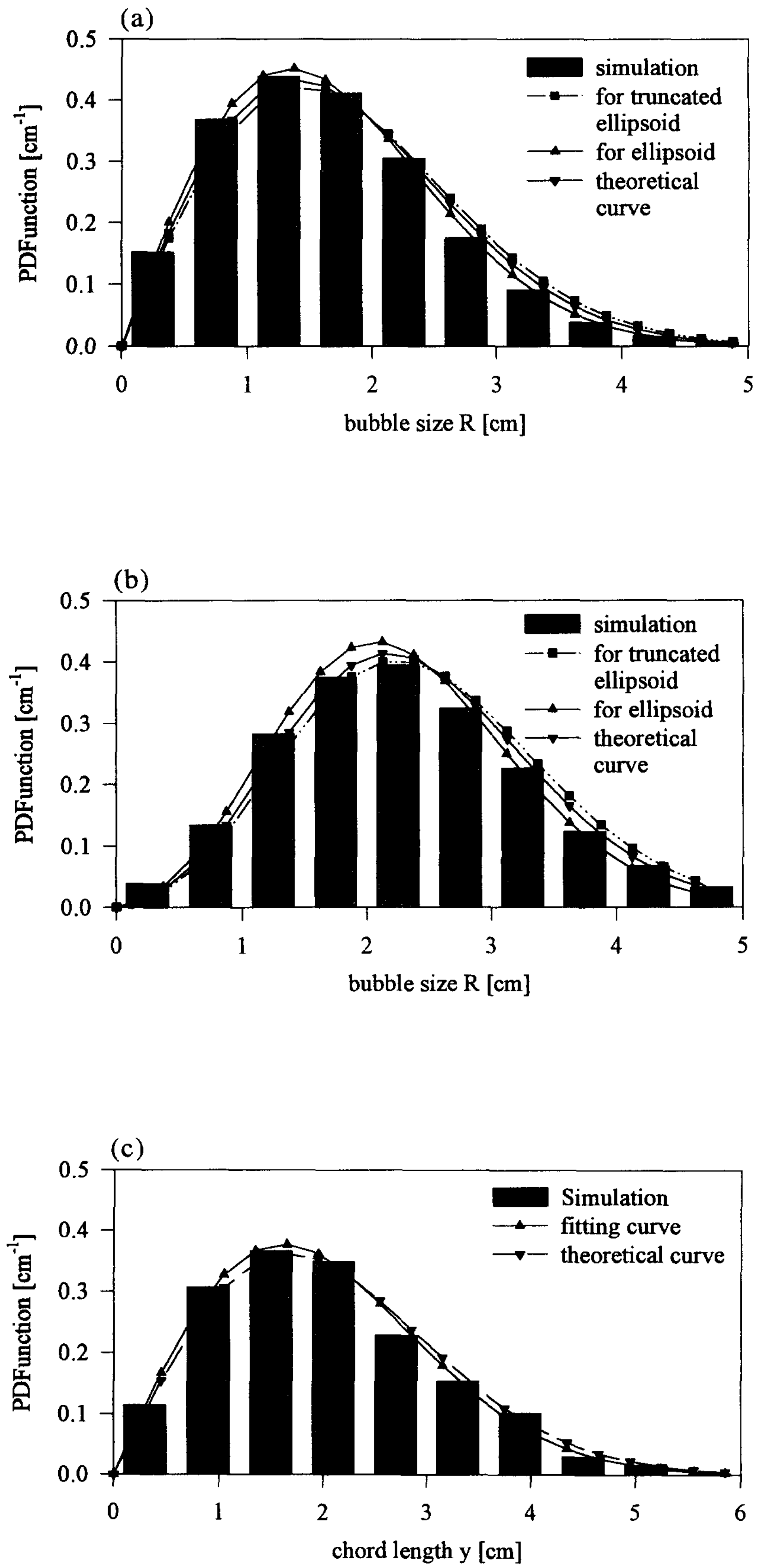

Figure 6 (a), (b) and (c) *Caption opposite*

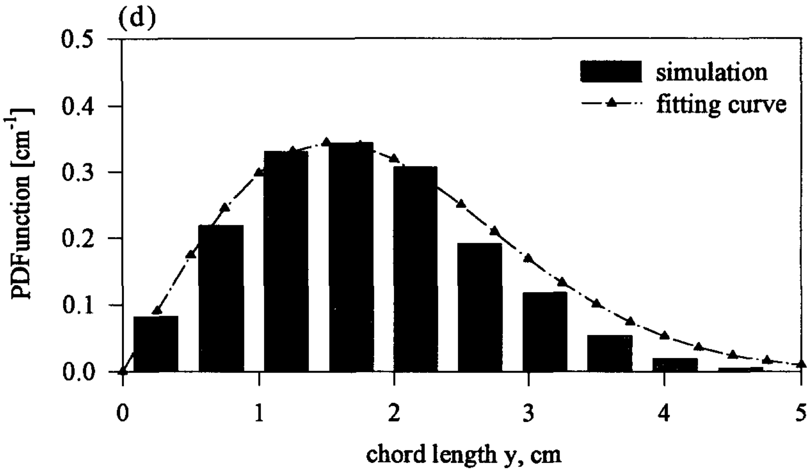

Figure 6(d)

Figure 6. Distributions of bubble sizes and chord lengths simulated for a given size distribution of bubbles in the bed—the Rayleigh probability function with parameter $\mu = 1.4$ and bubble shape factor $\alpha = 0.6$ for either ellipsoidally shaped bubbles or truncated ellipsoidally shaped bubbles with the truncation coefficient $K = 0.8$. The curves refer to the illusrated example toward the end of the paper. (a) Size distribution of bubbles in the bed; (b) size distribution of bubbles touching the proble; (c) distribution of chord lengths of ellipsoidally shaped bubbles; (d) distribution of chord lengths of truncated ellipsoidally shaped bubbles.

shaped bubbles and truncated ellipsoidally shaped bubbles with the truncation coefficient $K = 0.8$. Table 1 shows that the simulation data are very close to the theoretical data. From simulation data, it is easy to find that relationships of means and standard deviations between bubble sizes and chord lengths are in concord with [23] to [26].

In order to verify [23] to [26], means and standard deviations of sizes of bubbles touching the probe were calculated from those equations. We can see these values are very close to their theoretical or simulation values as shown in table 2.

Table 1. Means and standard deviations of sizes of bubbles with shape factor $\alpha = 0.6$ in the bed and touching the probe, and of chord lengths for both ellipsoidally shaped bubbles and truncated ellipsoidally shaped bubbles with the truncation coefficient $K = 0.8$, based on $P_s(R)$ is a Gamma distribution with parameters $\lambda = 2.8$ and $q = 4$, and a Rayleigh distribution with parameter $\mu = 1.4$, respectively

	M_s theoetical value	M_s simulation value	Relative error	M_{pR} theoretical value	M_{pR} simulation value	Relative error
Gamma distribution	1.4290	1.4330	0.28%	2.1428	2.1031	−1.85%
Rayleigh distribution	1.7546	1.7631	0.48%	2.6310	2.6236	−0.28%
	M_{cye} theoretical value	M_{cye} simulation value	Relative error	M_{cyt} theoretical value	M_{cyt} simulation value	Relative error
Gamma distribution	1.7142	1.7102	−0.23%	1.5360	1.5266	−0.61%
Rayleigh distribution	2.1056	2.1153	0.46%	1.8859	1.8882	0.12%
	σ_s theoretical value	σ_s simulation value	Relative error	σ_{pR} theoretical value	σ_{pR} simulation value	Relative error
Gamma distribution	0.7143	0.7140	−0.03%	0.8748	0.9085	3.85%
Rayleigh distribution	0.9172	0.9258	0.94%	0.9553	0.9608	0.58%
	σ_{cye} theoretical value	σ_{cye} simulation value	Relative error	σ_{cyt} theoretical value	σ_{cyt} simulation value	Relative error
Gamma distribution	0.9584	1.0025	4.60%	0.7962	0.8301	5.35%
Rayleigh distribution	1.1006	1.1138	1.20%	0.9062	0.9118	0.62%

Table 2. Means and standard deviations of size distributions of bubbles touching the probe which are found from means and standard deviations of chord lengths for either ellipsoidally shaped bubbles by using [23] and [24] or truncated ellipsoidally shaped bubbles by using [25] and [26]

	M_{pR} calculated from [23]	Relative error to theoretical	Relative error to simulation	M_{pR} calculated from [25]	Relative error to theoretical	Relative error to simulation
Gamma distribution	2.1378	−0.23%	1.65%	2.1297	−0.61%	1.26%
Rayleigh distribution	2.6441	0.49%	0.78%	2.6342	0.12%	0.40%
	σ_{pR} calculated from [24]	Relative error to theoretical	Relative error to simulation	σ_{pR} calculated from [26]	Relative error to theoretical	Relative error to simulation
Gamma distribution	0.9424	7.72%	3.73%	0.9320	6.54%	2.59%
Rayleigh distribution	0.9727	1.82%	1.24%	0.9644	0.95%	0.37%

Translation from distribution of chord lengths to distributions of bubble sizes

In practice, the true bubble size distribution is never (or rarely ever) known. However, the distribution of chord lengths can be measured in practice. The mean and standard deviation of $P_p(R)$, size distribution of bubbles touching the probe is readily found from [23] to [26]. However, deducing the size distribution of bubbles touching the probe, $P_p(R)$ from the distribution of chord lengths, $P_p(y)$ is very important. The following analysis is based on the ellipsoidally shaped bubble model.

Assume $P_c(y)$ and $P_p(R)$ are continuous probability functions, differentiate both sides of [12] to yield,

$$P_c'(y) = \int_{y/2\alpha}^{\infty} \frac{1}{2\alpha^2 R^2} P_p(R)\,dR - \frac{y}{\alpha y^2} P_p(y/2\alpha)$$

and multiply both sides by y to yield,

$$yP_c'(y) = \int_{y/2\alpha}^{\infty} \frac{y}{2\alpha^2 R^2} P_p(R)\,dR - \frac{1}{\alpha} P_p(y/2\alpha)$$

The first term in the right side of the above equation equals $P_c(y)$ identically, so that

$$P_p(y/2\alpha) = \alpha(P_c(y) - yP_c'(y))$$

let $R = y/2\alpha$, so that

$$P_p(R) = \alpha(P_e(2\alpha R) - 2\alpha R P_c'(2\alpha R)) \qquad [27]$$

The importance of [27] is to translate the distribution of chord lengths to the size distribution of bubbles touching the probe in analytical form. The size distribution of bubbles in the bed system can then be readily found by using [8]. In other words, when the data of chord lengths measured by a probe are available, a certain type of probability function may be employed to fit the data to obtain $P_c(y)$, and then [27] is used to find $P_p(R)$, at last, $P_s(R)$ can be found by using [8]. An illustrative example is given below.

Illustrative example. Take the simulation data of chord lengths in figure 6(c) as measured data, the curve fitting technique, i.e. least squares best fit method is used to fit the data with a Rayleigh probability function. The parameter μ of the fitting Rayleigh function is found to be 1.61 [solid line curve in figure 6(c)], which is close to the original theoretical value 1.68 [dashed line curve in figure 6(c)]. Therefore, the fitting curve $P_c(y)$, the distribution of chord lengths can be written as,

$$P_c(y) = \frac{y}{1.61^2} e^{-y^2/2 \times 1.61^2}$$

then [27] is used to find the size distribution of bubbles touching the probe $P_p(R)$ from this $P_c(y)$ and $P_c'(y)$,

$$P_p(R) = \alpha\left(\frac{2\alpha R}{1.61^2}e^{-(2\alpha R)^2/2\times 1.61^2} - 2\alpha R\left(\frac{1}{1.61^2}e^{-(2\alpha R)^2/2\times 1.61^2} - \frac{2\alpha R}{1.61^2}\frac{2(2\alpha R)}{2\times 1.61^2}e^{-(2\alpha R)^2/2\times 1.61^2}\right)\right)$$

$$= \frac{R^3}{2\times(1.61/2\alpha)^4}e^{-R^2/2\times(1/61/2\alpha)^2}$$

Substituting $\alpha = 0.6$ into this equation, yields,

$$P_p(R) = \frac{R^3}{2\times 1.34^4}e^{-R^2/2\times 1.34^2}$$

$P_p(R)$ is plotted with solid line in figure 6(b), which is very close to the original size distribution of bubbles touching the probe, $R^3\,e^{-R^2/2\times 1.4^2}/2\times 1.4^4$, the dashed line in the same figure. The mean and standard deivation of $P_p(R)$ are 2.5192 and 0.9144, respectiely, very close to the theoretical and simulation values in table 1.

The size distribution of bubbles in the bed, $P_s(R)$ can be found by using [8], that is,

$$P_s(R) = \frac{\dfrac{1}{R^2}\dfrac{R^3}{2\times 1.34^4}e^{-R^2/2\times 1.34^2}}{\displaystyle\int_0^\infty \frac{1}{R^2}\frac{R^3}{2\times 1.34^4}e^{-R^2/2\times 1.34^2}} = \frac{R}{1.34^2}e^{-R^2/2\times 1.34^2}$$

$P_s(R)$ is plotted in with solid line figure 6[a), which is very close to the original size distribution of bubbles in the bed, $R\,e^{-R^2/2\times 1.4^2}/1.4^2$, the dashed line in figure 6(a). The mean and standard deviation of $P_s(R)$ are 1.6794 and 0.8779, respectively, very close to the theoretical and simulation values in table 1.

For the truncated ellipsoidally shaped bubble model, [27] cannot be used directly unless the ellipsoidally shaped bubble is employed as an approximation of the truncated ellipsoidally shaped model. The determination of the shape factor of the ellipsoidally shape bubble model for approximating the truncated ellipsoidally shaped bubble model, is based on the fact that both models have the same average bubble size for a set of chord lengths, that is,

$$\frac{3}{4\alpha_{app}}M_{cy} = \left(\frac{1}{\frac{2}{3}\alpha(1+Q)^3 - \alpha Q(1+Q)^2}\right)M_{cy}$$

so that,

$$\alpha_{app} = \tfrac{1}{4}(2\alpha + 3\alpha Q - \alpha Q^3) \qquad [28]$$

When α_{app} is known, [27] can be used to find the bubble size distributions. For instance, take the simulation data of chord lengths in figure 6(d) as measured data, where the bubble shape factor α is 0.6 and the truncated coefficient Q is 0.6, and substitute α and Q into [28], so that the approximate shape factor is 0.5376. Thus, $P_c(y)$ is found with the same technique described above to be $y\,e^{-y^2/2\times 1.55^2}/2\times 1.55^2$, and is illustrated in figure 6(d). Equations [27] and [8] are used to find size distributions $P_p(R)$ and $P_s(R)$, respectively, that is,

$$P_p(R) = \frac{R^3}{2\times 1.44^4}e^{-R^2/2\times 1.44^2}$$

$$P_s(R) = \frac{R}{1.44^2}e^{-R^2/2\times 1.44^2}$$

which are illustrated in figure 6(a) and (b). Results show that $P_s(R)$ and $P_p(R)$ are in good agreement with their original distributions.

The above example shows that the approach is feasible and powerful. The results are shown to agree with the forward transform. Generally, the accuracy of the method relies on the measured data and selection of a probability function to fit the data.

CONCLUSIONS

The relationships between distributions of bubble sizes and distributions of chord lengths are discussed extensively in this paper. The analyses indicate that means and standard deviations of chord lengths and bubble sizes are related to each other unequivocally and are not dependent on the nature of their distributions. The quantitative relationships between the mean and standard deviation of chord lengths and mean and standard deviation of bubble sizes can be described by [23] and [24] for ellipsoidally shaped bubbles and by [25] and [26] for truncated ellipsoidally shaped bubbles. In measurement, the probe favors a larger average size of bubbles than the average size in the bed system. Those analyses are verified by the simulation. The simulation and calculated results indicate that the develoepd analytic approach for transforming the distribution of chord lengths measured by the probe to the size distributions of bubbles touching the probe and in the bed is correct, feasible and powerful. The approach provided for the first time is in a closed form and can quickly and effectively process measured data.

Acknowledgement—The authors are grateful for support of this research to the National Science Foundation, Grant No. CTS-8957146.

REFERENCES

Atkinson, C. M. & Clark, N. N. 1986a Analysis of fluidized bed behavior using probes. In *Proceedings, 11th Power Bulk Solid Conf.*, Rosemont, IL, pp. 437–443.

Atkinson, C. M. & Clark, N. N. 1986b A gas sampling system for high temperature fluidized bed. In *Proceedings, 11th Power Bulk Solid Conf.*, Rosemont, IL, pp. 444–454.

Burgess, J. M., Fane, A. G. & Fell, C. J. D. 1981 Application of an electroresistivity probe techniques to a two dimensional fluidized bed. *Trans. Inst. Chem. Engrs* **60,** 249–252.

Chan, L. H., Sishtla, C. & Knowlton, T. M. 1987 The effect of pressure on bubble parameters in gas-fluidized beds. *Powder Technol.* **53,** 217–235.

Cheremisinoff, N. P. 1986 Review of experimental methods for studying hydrodynamics of gas–solid fluidized bed. *Ind. Engng Chem. Process. Des. Dev.* **25,** 329–351.

Clark, N. N. & Turton, R. 1988 Chord length distributions related to bubble size distributions in multiphase flows. *Int. J. Multiphase Flow* **14,** 413–424.

Epstein, N. 1981 Three phase fluidization: some knowledge gaps. *Can. J. Chem. Engng* **51,** 649–657.

Gunn, D. J. & Al-doori, H. H. 1985 The measurement of bubble flows in fluidized beds by electrical probe. *Int. J. Multiphase Flow* **11,** 535–551.

Lee, S., Soria, A. & Lasa, H. 1990 Evolution of bubble length distributions in three-phase fluidized beds. *AIChE Jl* **36,** 1763–1767.

Lim, K. S., Agarwal, P. K. & O'Neill, B. K. 1990a Measurement and modeling of bubble parameters in a two-dimensional gas-fluidized bed using image analysis. *Powder Technol.* **60,** 159–171.

Lim, K. S. & Agarwal, P. K. 1990b Conversion of pierced lengths measured at a probe to bubble size measures: an assessment of the geometrical probability approach and bubble shape models. *Powder Technol.* **63,** 205–219.

Matsuura, A. & Fan, L. 1984 Distribution of bubble properties in a gas–liquid–solid fluidized bed. *AIChE Jl* **30,** 894–903.

Meernik, P. R. & Yuen, M. C. 1988a An optical method for determining bubble size distribution—Part I: theory. *J. Fluids Engng* **11,** 325–331.

Meernik, P. R. & Yuen, M. C. 1988b An optical method for determining bubble size distribution—Part II: application to bubble size measurement in a three phase fluidized bed. *J. Fluids Engng* **11,** 332–338.

Turton, R. & Clark, N. N. 1989 Interpreting probe signals from fluidized beds. *Powder Technol* **59,** 117–123.

Weimer, A. W., Gyure, D. D. & Clough, D. E. 1985 Application of a Gamma-radiation density gauge for determining hydrodynamic properties of fluidized beds. *Powder Technol.* **44,** 179–194.

Werther, J. 1974a Bubbles in gas fluidized beds—Part I. *Trans. Inst. Chem. Engrs* **52,** 149–159.

Werther, J. 1974b Bubbles in gas fluidized beds—Part II. *Trans. Inst. Chem. Engrs* **52,** 160–169.
Werther, J. & Molerus, O. 1973 The local structure of gas fluidized beds I. A statistically based measuring system. *Int. J. Multiphase Flow* **1,** 101–122.